Available online at www.sciencedirect.com
ScienceDirect
Biochemical and Biophysical Research Communications 361 (2007) 116–121
BBRC
www.elsevier.com/locate/ybbrc

Aurones serve as probes of β-amyloid plaques in Alzheimer's disease

Masahiro Ono [a,*], Yoshifumi Maya [a], Mamoru Haratake [a], Kazuhiro Ito [b], Hiroshi Mori [b], Morio Nakayama [a]

[a] Department of Hygienic Chemistry, Graduate School of Biomedical Sciences, Nagasaki University, 1-14 Bunkyo-machi, Nagasaki 852-8521, Japan
[b] Department of Neuroscience, Osaka City University Medical School, 1-4-3 Asahi-machi, Abeno-ku, Osaka 545-8585, Japan

Received 21 June 2007
Available online 10 July 2007

Abstract

A novel series of aurone derivatives for *in vivo* imaging of β-amyloid plaques in the brain of Alzheimer's disease (AD) were synthesized and characterized. When *in vitro* binding studies using Aβ(1−42) aggregates were carried out with aurone derivatives, they showed high binding affinities for Aβ(1−42) aggregates at the K_i values ranging from 1.2 to 6.8 nM. When *in vitro* plaque labeling was carried out using double transgenic mice brain sections, the aurone derivatives intensely stained β-amyiloid plaques. Biodistribution studies in normal mice after i.v. injection of the radioiodinated aurones displayed high brain uptake (1.9–4.6% ID/g at 2 min) and rapid clearance from the brain (0.11–0.26% ID/g at 60 min), which is highly desirable for amyloid imaging agents. The results in this study suggest that novel radiolabeled aurones may be useful amyloid imaging agents for detecting β-amyloid plaques in the brain of AD.

Keywords: Amyloid; SPECT; PET; Aurone

Alzheimer's disease (AD), the most common senile dementia, is characterized by β-amyloid plaques, vascular amyloid, neurofibrillary tangles, and progressive neurodegeneration [1,2]. The formation of β-amyloid plaques, composed of β-amyloid (Aβ) peptides, in the brain is considered to be an initial neurodegenerative event in AD. Thus, the detection of individual Alzheimer's amyloid plaques *in vivo* by single photon emission tomography (SPECT) or positron emission tomography (PET) should improve diagnosis and also accelerate discovery of effective therapeutic agents for AD [3,4].

Many radiolabeled amyloid imaging probes based on DDNP, Congo Red, and thioflavin T have been reported previously. Among them, [^{18}F]FDDNP [5,6], [^{11}C]PIB [7,8], [^{11}C]SB-13 [9,10], [^{123}I]IMPY [11,12] and [^{11}C]BF-227 [13] have been tested clinically and have demonstrated the potential utility of *in vivo* imaging of amyloid plaques in the brain. However, few core structures for amyloid imaging probes have been found other than DDNP, Congo Red and thioflavin T.

Recently, we have reported that radioiodinated flavones function as a new backbone structure in the development of amyloid imaging probes (Fig. 1) [14]. The flavones derivatives showed good binding affinity to Aβ aggregates and high brain penetration, but slow clearance from the brain was also observed, resulting in low background-to-noise ratios.

To explore more useful candidates of core structures for amyloid imaging probes, we selected one of the flavonoids, aurone, as a new core structure (Fig. 1) [15]. In the present study, we synthesized a series of aurone derivatives, which possess a radioiodine at 5 position and a nucleophilic group (NH_2, NHMe, NMe_2) at 4′ position, and evaluated their biological activities as *in vivo* amyloid imaging agents. To our knowledge, this is the first report in which aurone derivatives have been applied as amyloid imaging agents for detecting AD.

* Corresponding author. Fax: +81 95 819 2442.
E-mail address: mono@nagasaki-u.ac.jp (M. Ono).

0006-291X/$ - see front matter © 2007 Elsevier Inc. All rights reserved.
doi:10.1016/j.bbrc.2007.06.162

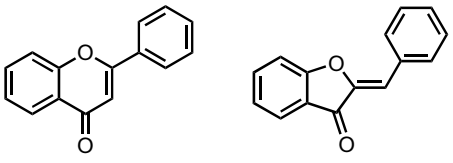

Fig. 1. Chemical structures of flavone and aurone.

Materials and methods

All reagents used in syntheses were commercial products and were used without further purification unless otherwise indicated. ^{1}H NMR spectra were obtained on a Varian Gemini 300 spectrometer with TMS as an internal standard. Coupling constants are reported in Hertz. Multiplicity was defined by s (singlet), d (doublet), t (triplet), br (broad), and m (multiplet). Mass spectra were obtained on a JEOL IMS-DX instrument.

Chemistry. 2-(2-Methoxy-2-oxoethoxy)-5-bromobenzoic acid methyl ester (**1**). To a solution of 2-hydroxy-5-bromobenzoic acid methyl ester (1.5 g, 6.49 mmol) in acetone (10 mL) was added K_2CO_3 (2.7 g, 19.5 mmol) and ethylbromoacetate (1.3 mL, 7.78 mmol). The mixture was stirred for 3 h under reflux. After evaporating the solvent, the residue was dissolved in water (100 mL) and extracted with ethyl acetate (100 mL). The organic layer was dried over Na_2SO_4, and evaporation of solvent gave 1.60 g of **1** (77.7%). ^{1}H NMR (300 MHz, $CDCl_3$) δ 1.29 (t, $J = 7.2$ Hz, 3H), 3.91 (s, 3H), 4.24 (q, $J = 7.2$ Hz, 2H), 4.69 (s, 2H), 6.78 (d, $J = 9.0$ Hz, 1H), 7.54 (d, $J = 6.3$ Hz, 1H), 7.96 (s, 1H) .

2-(Carboxymethoxy)-5-bromobenzoic acid (**2**). To a solution of **1** (1.60 g, 5.04 mmol) in methanol (10 mL) was added 10% aqueous KOH (3.0 mL). The mixture was stirred for 2 h at room temperature. The product formed by adding of 1 N HCl was filtered to give 1.10 g of **2** (79.4%).

5-Bromo-3-acetoxybenzofuran (**3**). A mixture of acetic anhydride (20 mL), acetic acid (4 mL), anhydrous sodium acetate (1.0 g, 12.0 mmol), and **2** (100 mg, 0.36 mmol) was heated to reflux for 5 h. Water (100 mL) was then added, and the mixture was extracted with chloroform (100 mL). After drying of the organic layer on Na_2SO_4, evaporation gave 78 mg of **3** (86.5%). ^{1}H NMR (300 MHz, $CDCl_3$) δ 2.37 (s, 3H), 7.33 (d, $J = 9.0$ Hz, 1H), 7.43 (dd, $J = 3.6$, 2.1 Hz, 1H), 7.71 (s, 1H), 8.02 (s, 1H).

5-Bromo-3(2H)-benzofuranone (**4**). A mixture of **3** (78 mg, 0.31 mmol), methanol (3 mL), water (1 mL), and 1 N HCl (2 mL) was heated to reflux for 3 h. The precipitate formed was collected by filtration, washed with water, and dried under vacuum to obtain 15 mg of **4** (22.5%). ^{1}H NMR (300 MHz, $CDCl_3$) δ 4.67 (s, 2H), 7.06 (d, $J = 9.0$ Hz, 1H), 7.69 (dd, $J = 2.1$, 2.1 Hz, 1H), 7.79 (d, $J = 2.1$ Hz, 1H).

5-Bromo-2-[(4-nitrophenyl)methylene]-3(2H)-benzofuranone (**5**). To a solution of **4** (200 mg, 0.94 mmol) and 4-nitrobenzaldehyde (171 mg, 1.13 mmol) in chloroform (5 mL) was added Al_2O_3 (2.7 g, 26.0 mmol). The mixture was stirred for 20 min at room temperature. After filtration of the reaction mixture, the solvent of the filtrate was removed, and drying under vacuum yielded 142 mg of **5** (43.7%).

2-[(4-Aminophenyl)methylene]-5-bromo-3(2H)-benzofuranone (**6**). A mixture of **5** (10 mg, 0.028 mmol), $SnCl_2$ (0.64 g, 2.37 mmol) and ethanol (10 mL) was stirred under reflux for 2 h. After the mixture was cooled to room temperature, 1 M NaOH (100 mL) was added and extracted with ethyl acetate (100 mL). The organic layer was dried over Na_2SO_4 and filtered. The filtrate was concentrated to give 7.0 mg of **6** (79.1%). ^{1}H NMR (300 MHz, $CDCl_3$) δ 4.11 (s, 2H), 6.72 (d, $J = 8.7$ Hz, 2H), 6.90 (s, 1H), 7.23 (d, $J = 8.4$ Hz, 1H), 7.70 (dd, $J = 2.1$, 2.1 Hz, 1H), 7.76 (d, $J = 8.4$ Hz, 2H), 7.92 (d, $J = 1.8$ Hz, 1H).

5-Bromo-2-[(4-methylaminophenyl)methylene]-3(2H)-benzofuranone (**7**). To a solution of **6** (100 mg, 0.316 mmol) in DMSO (5 mL) was added methyl iodine (0.15 mL, 2.40 mmol) and anhydrous K_2CO_3 (380 mg, 2.75 mmol). The reaction mixture was stirred at 50 °C for 3 h. After water (100 mL) was added, the mixture was extracted with ethyl acetate (100 mL). The organic layer was dried over Na_2SO_4. Evaporation of the solvent afforded a residue, which was purified by preparative TLC (1:2 ethyl acetate/hexane) to give 49 mg of **7** (47.5%). ^{1}H NMR (300 MHz, $CDCl_3$) δ 2.92 (s, 3H), 4.21 (s, 1H), 6.59 (d, $J = 8.7$ Hz, 2H), 6.92 (s, 1H), 7.25 (d, $J = 8.7$ Hz, 1H), 7.68 (dd, $J = 2.1$, 2.1 Hz, 1H), 7.78 (d, $J = 8.7$ Hz, 2H), 7.91 (d, $J = 2.1$ Hz, 1H).

5-Bromo-2-[(4-dimethylaminophenyl)methylene]-3(2H)-benzofuranone (**8**). The same reaction described above to prepare **5** was used, and 42 mg of **8** was obtained in a 51.9% yield from **4**. ^{1}H NMR (300 MHz, $CDCl_3$) δ 3.09 (s, 6H), 6.70 (d, $J = 11.4$ Hz, 2H), 6.95 (s, 1H), 7.22 (d, $J = 8.7$ Hz, 1H), 7.67 (d, $J = 9.6$ Hz, 1H), 7.83 (d, $J = 9.0$ Hz, 2H), 7.92 (d, $J = 2.1$ Hz, 1H).

2-[(4-Aminophenyl)methylene]-5-tributylstannyl-3(2H)-benzofuranone (**9**). A mixture of **6** (78 mg, 0.25 mmol), $(Bu_3Sn)_2$ (0.4 mL) and $(Ph_3P)_4Pd$ (50 mg, 0.043 mmol) in a mixed solvent (10 mL, 1:1 dioxane/Et_3N) was stirred under reflux for 3 h. The solvent was removed, and the residue was purified by preparative TLC (1:2 ethylacetate/hexane) to give 30 mg of **9** (23.1%). ^{1}H NMR (300 MHz, $CDCl_3$) δ 0.86–1.57 (m, 27H), 4.05 (s, 2H), 6.73 (d, $J = 8.7$ Hz, 2H), 6.87 (s, 1H), 7.30 (d, $J = 8.1$ Hz, 1H), 7.69 (dd, $J = 0.6$, 0.9 Hz, 1H), 7.78 (d, $J = 8.4$ Hz, 2H), 7.89 (s, 1H).

2-[(4-Methylaminophenyl)methylene]-5-tributylstannyl-3(2H)-benzofuranone (**10**). The same reaction as described above to prepare **9** was used, and 28 mg of **10** was obtained in a 34.6% yield from **7**. ^{1}H NMR (300 MHz, $CDCl_3$) δ 1.06–1.57 (m, 27H), 3.12 (s, 3H), 4.42 (s, 1H), 6.73 (d, $J = 8.7$ Hz, 2H), 7.10 (s, 1H), 7.49 (d, $J = 8.1$ Hz, 1H), 7.88 (dd, $J = 1.2$, 1.2 Hz, 1H), 8.01 (d, $J = 8.7$ Hz, 2H), 8.09 (s, 1H).

2-[(4-Dimethylaminophenyl)methylene]-5-tributylstannyl-3(2H)-benzofuranone (**11**). The same reaction as described above to prepare **9** was used, and 7 mg of **11** was obtained in a 35.2% yield from **8**. ^{1}H NMR (300 MHz, $CDCl_3$) δ 0.86–1.57 (m, 27H), 3.07 (s, 6H), 6.75 (d, $J = 9.0$ Hz, 2H), 6.92 (s, 1H), 7.29 (d, $J = 7.2$ Hz, 1H), 7.67 (dd, $J = 1.2$, 0.9 Hz, 1H), 7.86 (d, $J = 9.0$ Hz, 2H), 7.95 (s, 1H).

2-[(4-Aminophenyl)methylene]-5-iodo-3(2H)-benzofuranone (**12**). To a solution of **9** (30 mg, 0.057 mmol) in chloroform (3 mL) was added a solution of iodine in chloroform (1 mL, 0.25 M) at room temperature. The mixture was stirred at room temperature for 10 min, and saturated $NaHSO_3$ solution (15 mL) was added. The organic layer was separated, dried over Na_2SO_4 and filtered. The solvent was removed, and the residue was purified by preparative TLC (1:2 ethyl acetate/hexane) to give 14 mg of **12** (67.6%). ^{1}H NMR (300 MHz, $CDCl_3$) δ 4.10 (s, 2H), 6.72 (d, $J = 8.7$ Hz, 2H), 6.90 (s, 1H), 7.13 (d, $J = 9.0$ Hz, 1H), 7.76 (d, $J = 8.4$ Hz, 2H), 7.87 (d, $J = 10.5$ Hz, 1H), 8.11 (s, 1H) . MS m/z 363 [M^+].

5-iodo-2-[(4-methylaminophenyl)methylene]-3(2H)-benzofuranone (**13**). The same reaction described above to prepare **12** was used, and 10 mg of **13** was obtained in a 48.2% yield from **10**. ^{1}H NMR (300 MHz, $CDCl_3$) δ 2.92 (s, 3H), 4.27 (s, 1H), 6.64 (d, $J = 9.0$ Hz, 2H), 6.90 (s, 1H), 7.12 (d, $J = 8.4$ Hz, 1H), 7.79 (d, $J = 8.7$ Hz, 2H), 7.86 (dd, $J = 2.1$, 2.1 Hz, 1H), 8.11 (d, $J = 2.1$ Hz, 1H). MS m/z 377 [M^+].

2-[(4-Dimethylaminophenyl)methylene]-5-iodo-3(2H)-benzofuranone (**14**). The same reaction described above to prepare **12** was used, and 3 mg of **14** was obtained in a 63.9% yield from **11**. ^{1}H NMR (300 MHz, $CDCl_3$) δ 3.08 (s, 6H), 6.74 (d, $J = 9.0$ Hz, 2H), 6.95 (s, 1H), 7.12 (d, $J = 8.7$ Hz, 1H), 7.82-7.88 (m, 3H), 8.12 (s, 1H). MS m/z 391 [M^+].

Iododestannylation reaction. The radioiodinated forms of compounds **12**, **13**, and **14** were prepared from the corresponding tributyltin derivatives by an iododestannylation according to the procedure previously reported [14]. The radioiodinated ligand was purified by HPLC on a Cosmosil C18 column with an isocratic solvent of H_2O/acetonitrile (3:7) at a flow rate of 1.0 mL/min.

Binding assays using the aggregated Aβ peptide in solution. A solid form of Aβ(1–42) was purchased from Peptide Institute (Osaka, Japan). Aggregation of peptides was carried out by gently dissolving the peptide (0.25 mg/mL) in a buffer solution (pH 7.4) containing 10 mM sodium phosphate and 1 mM EDTA. The solutions were incubated at 37 °C for 42 h with gentle and constant shaking. Binding studies were carried out according to the procedure described previously [14]. Values for the half-maximal inhibitory concentration (IC_{50}) were determined from displacement curves of three independent experiments using GraphPad Prism 4.0,

and those for the inhibition constant (K_i) were calculated using the Cheng-Prusoff equation[16]: $K_i = IC_{50}/(1 + [L]/K_d)$, where $[L]$ is the concentration of [^{125}I]**12** used in the assay, and K_d is the dissociation constant of compound **12**.

Staining of amyloid plaques in double transgenic mice brain sections. Double transgenic mice (6 month of age) produced by Tg2576 crossed with mutated PS1 (A260V) mice were used as Alzheimer's model mice. Brain tissues were obtained and fixed with 10% formaldehyde. Dehydrated tissues with ethanol and xylene were paraffinized and the resultant wax blocks were sliced into serial sections of 5-μm thickness. The tissue slides were deparaffinized with xylene, ethanol, and distilled water. After incubation with PBS for 30 min, each slide was incubated with 50% ethanol solution (100 μM) of compound **14**. Finally, the sections were washed in PBS for 15 min. Thereafter, the sections were incubated in ethanol and xylene, and embedded in Entellan Neu (Merck, Darmstadt, Germany). Fluorescent observation was performed by the Leica TCS SP2 system with a DMIRE2 fluorescence microscope. Staining with compound **14** was detected using a filter set with 458 nm exicitation and 540–580 nm emission. The same sections were also immunostained with DAB as a chromogen using monoclonal antibodies against β-amyloid as previously reported [17].

In vivo biodistribution in normal mice. Animal studies were conducted in accordance with our institutional guidelines and were approved by Nagasaki University Animal Care Committee. A saline solution (100 μL) containing radiolabeled agents (4.2–6.3 kBq) and 10% ethanol was injected directly into the tail vein of ddY mice (5-week-old, average weight 20–25 g). The mice were sacrificed at various time points post injection. The organs of interest were removed and weighed, and the radioactivity was counted with an automatic gamma counter (Aloka, ARC-380).

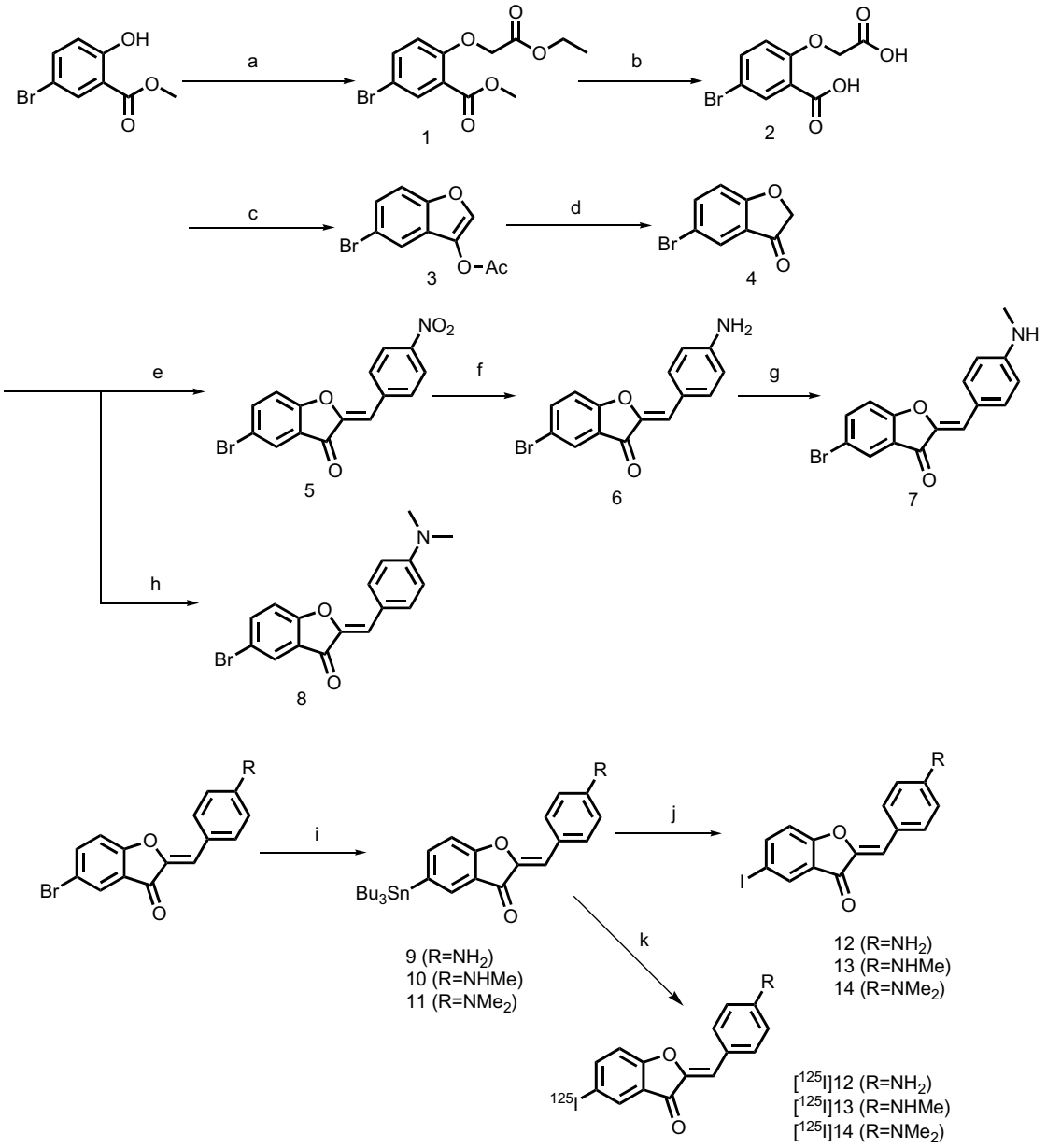

Fig. 2. Synthetic route of aurone derivatives. (a) acetone, ethylbromoacetate, K_2CO_3, (b) NaOH, (c) AcONa, Ac_2O, AcOH, (d) MeOH, HCl, H_2O, (e) 4-nitrobenzaldehyde, Al_2O_3, $CHCl_3$, (f) $SnCl_2$, EtOH, (g) MeI, K_2CO_3, DMSO, (h) 4-dimethylaminobenzaldehyde, Al_2O_3, $CHCl_3$, (i) dioxane, $(Bu_3Sn)_2$, $(Ph_3P)_4Pd$, Et_3N, (j) $CHCl_3$, I_2, (k) [^{125}I]NaI, HCl, H_2O_2.

Results and discussion

Chemistry

The target aurone derivatives (**12**, **13**, and **14**) were prepared as shown in Fig. 2. The synthesis of aurone backbone was achieved by Aldol reaction of benzofuranones with benzaldehydes using Al_2O_3. In this process, 5-bromo-3-benzofuranone was reacted with 4-nitrobenzaldehyde or 4-dimethylaminobenzaldehyde in the presence of Al_2O_3 in chloroform at room temperature to form **5** and **8** in yields of 43.7% and 51.9%, respectively. The amino derivative **6** was readily prepared from **5** by reduction with $SnCl_2$ (79.1% yield). Conversion of **6** to the monomethylamino derivative **7** was achieved by a methylation with CH_3I under alkaline conditions (47.5% yield). The tributyltin derivatives (**9**, **10**, and **11**) were prepared from the corresponding bromo compounds (**6**, **7,** and **8**) using a bromo to tributyltin exchange reaction catalyzed by Pd(0) for yields of 23.1%, 34.6% and 35.2%, respectively. The tributyltin derivatives (**9**, **10,** and **11**) were readily reacted with iodine in chloroform at room temperature to give the iodo derivatives, compounds **12**, **13**, and **14** at yields of 67.6%, 48.2% and 63.9%, respectively. Furthermore, the tributyltin derivatives (**9**, **10**, and **11**) can also be used as the starting materials for radioiodination in preparation of [^{125}I]**12**, [^{125}I]**13**, and [^{125}I]**14**. Novel radioiodinated aurones were achieved by an iododestannylation reaction using hydrogen peroxide as the oxidant, which produced the desired radioiodinated ligands. It was anticipated that the no-carrier-added preparation would result in a final product bearing a theoretical specific activity similar to that of ^{125}I (2200 Ci/mmol). The radiochemical identities of the radioiodinated ligands were verified by co-injection with nonradioactive compounds by their HPLC profiles. The final radioiodinated compounds [^{125}I]**12**, [^{125}I]**13,** and [^{125}I]**14** showed a single radioactivity peak at retention times of 4.4, 7.1 and 11.8 min, respectively. Three radioiodinated products were obtained in 36–54% radiochemical yields with radiochemical purities of >95% after purification by HPLC.

Binding studies using Aβ aggregates in vitro

To evaluate the binding affinity of aurone derivatives to Aβ aggregates, saturation assay with [^{125}I]**12** was carried out using Aβ(1–42) aggregates. When the saturation bindings of [^{125}I]**12** were transformed to Scatchard plots, they showed linear plots, indicating that aurone derivatives have one binding site on Aβ aggregates (Fig. 3). [^{125}I]**12** displayed excellent binding affinity for Aβ(1–42) aggregates at K_d of 7.9 ± 1.3 nM. Binding affinities of nonradioactive aurones (**12**, **13**, and **14**) were also evaluated with inhibition studies against [^{125}I]**12** binding on Aβ(1–42) aggregates (Table 1). The K_i values estimated for **12**, **13,** and **14** were 2.7, 1.2, and 6.8 nM for Aβ(1–42) aggregates, respectively. These K_i values suggested that the new series of aurones

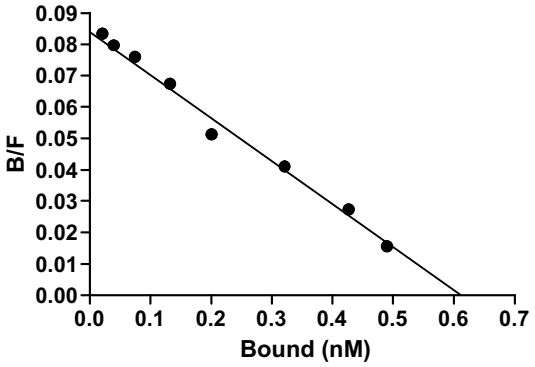

Fig. 3. Scatchard plots of [^{125}I]**12** binding to Aβ(1–42) aggregates. High binding affinity with a K_d value in a nanomolar range was obtained ($K_d = 7.9 \pm 1.3$ nM).

Table 1
Inhibition constants of aurone derivatives on ligand binding to Aβ(1–42) aggregates

Compound	K_i (nM)[a]
12	2.69 ± 0.16
13	1.24 ± 0.11
14	6.82 ± 0.48

[a] Values are means ± standard error of the mean of three independent experiments.

had excellent binding affinity for Aβ(1–42) aggregates, and showed considerable tolerance for structural modification. Comparing these K_i values with the radioiodinated flavones reported previously, the K_i values of the radioiodinated aurones were lower than those of the radioiodinated flavones, indicating that the radioiodinated aurones have higher binding affinities to β-amyloid plaques than those of the corresponding radioiodinated flavones. Moreover, this finding suggests that the radioiodinated aurones with high binding affinities to Aβ(1–42) aggregates can detect diffuse plaques mainly composed of Aβ(1–42), which are considered to be the initial neuropathological change in AD brains.

Neuropathological staining on Alzheimer's model mouse brain sections

To confirm the binding affinity of aurone derivatives to β-amyloid plaques in the brain, neuropathological flurorescent staining with compound **14** was carried out using double transgenic Alzheimer's mouse brain sections (Fig. 4). Many β-amyloid plaques are clearly stained with compound **14**, as reflected by the high binding affinity to Aβ aggregates on *in vitro* competition assays. The compound clearly stained not only core plaques, but also typical senile plaques. The labeling pattern was consistent with that observed by immunohistochemical labeling with an antibody specific for Aβ, indicating that aurone derivatives show specific binding to β-amyloid plaques. Thus, the

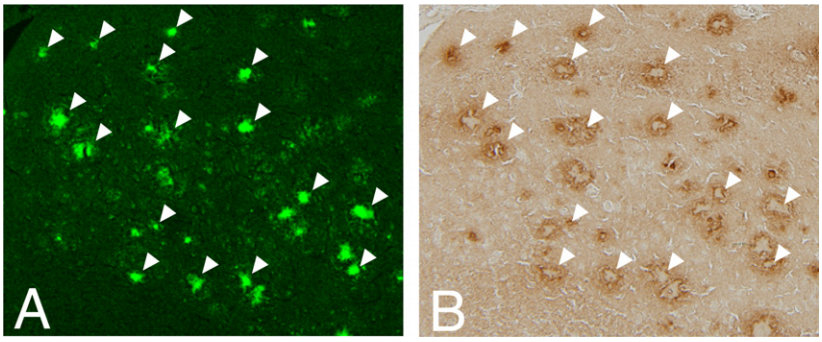

Fig. 4. Neuropathological staining of compound **14** on 5 μm AD model mouse sections from the cortex. (A) Many amyloid plaques are clearly stained with compound **14**. (B) The same sections were immunostained using an antibody against β-amyloid.

results suggest that aurone derivatives may be applicable for *in vivo* imaging of amyloid plaques in the brain.

Biodistribution studies

To evaluate brain uptake of the aurone derivatives, *in vivo* biodistribution studies in normal mice were performed with three radioiodinated aurones ([^{125}I]**12**, [^{125}I]**13**, and [^{125}I]**14**) (Table 2). The aurone derivatives displayed high brain uptakes raging from 1.9–4.6% ID/g brain at 2 min postinjection, indicating a level sufficient for amyloid imaging in the brain. In addition, they displayed rapid clearance from the normal brain with 0.49%, 0.32%, and 0.26% ID/g at 30 min postinjection for [^{125}I]**12**, [^{125}I]**13,** and [^{125}I]**14**, respectively. These values were equal to 10.7%, 10.1% and 13.8% of initial brain uptake peak for [^{125}I]**12**, [^{125}I]**13**, and [^{125}I]**14**, respectively. We previously reported that radioiodinated flavones showed high brain uptake (3.2–4.1% ID/g at 2 min postinjection) and good clearance from the brain (0.5–1.9% ID/g at 30 min postinjection). However, the ratios of 2 min to 30 min mouse brain uptake of the radioiodinated flavones were 40.0%, 44.6%, and 57.8% for NH_2, NHMe and NMe_2 derivatives, respectively, which were higher than those of radioiodinated aurones. When *ex vivo* autoradiography using [^{125}I]**14** was also performed, the radioactivity accumulated in the brain at 2 min postinjection rapidly eliminated from the normal mouse brain, and no marked radioactivity was observed in the brain at 30 min postinjection (included in Supplementary data). The result suggests that aurone derivatives do not show high non-specific binding in the brain *in vivo*. Since no Aβ plaques exist in the normal mouse brain, the washout of probes from the brain should be rapid to obtain a higher signal-to-noise ratio earlier in the AD brain. Therefore, these desirable pharmacokinetics demonstrated by radioiodinated aurones are critical to detect amyloid plaques in the AD brain. These biodistribution data suggest that novel radioiodinated aurones may have more suitable *in vivo* pharmacokinetic properties for amyloid imaging in AD brains compared with the radioiodinated flavones.

Table 2
Biodistribution of radioactivity after intravenous administration of [^{125}I]**12**, [^{125}I]**13**, and [^{125}I]**14** in mice[a]

Compound	Time after Injection (min)			
	2	10	30	60
[^{125}I]**12**	4.57	1.51	0.49	0.26
	(0.27)	(0.17)	(0.06)	(0.03)
[^{125}I]**13**	3.17	1.22	0.32	0.24
	(0.45)	(0.09)	(0.02)	(0.03)
[^{125}I]**14**	1.89	0.69	0.26	0.11
	(0.38)	(0.21)	(0.04)	(0.03)

[a] Expressed as % injected dose per gram. Each value represents mean (SD) for five mice at each interval.

Conclusion

In conclusion, we successfully designed and synthesized a new series of aurone derivatives as probes for *in vivo* imaging of amyloid plaques in the brain. In the *in vitro* binding studies, these aurones showed high binding affinity to Aβ(1–42) aggregates. The aurone derivatives clearly stained amyloid plaques in AD model mice brains, reflecting high binding affinity to Aβ aggregates *in vitro*. In biodistribution studies using normal mice, they displayed a good brain penetration and fast washout from the brain; highly desirable characteristics for *in vivo* amyloid imaging agents. Taken together, the present results suggest that the novel radioiodinated aurones may be useful probes for detecting amyloid plaques in the AD brain.

Acknowledgments

This work was supported in part by Industrrial Technology Research Grant Program in 2005 from New Energy and Industrial Technology Development Organization (NEDO) of Japan.

Appendix A. Supplementary data

Supplementary data associated with this article can be found, in the online version, at doi:10.1016/j.bbrc.2007.06.162.

References

[1] J.A. Hardy, G.A. Higgins, Alzheimer's disease: the amyloid cascade hypothesis, Science 256 (1992) 184–185.

[2] D.J. Selkoe, Alzheimer's disease: genes, proteins, and therapy, Physiol. Rev. 81 (2001) 741–766.

[3] C.A. Mathis, Y. Wang, W.E. Klunk, Imaging beta-amyloid plaques and neurofibrillary tangles in the aging human brain, Curr. Pharm. Des. 10 (2004) 1469–1492.

[4] A. Nordberg, PET imaging of amyloid in Alzheimer's disease, Lancet Neurol. 3 (2004) 519–527.

[5] K. Shoghi-Jadid, G.W. Small, E.D. Agdeppa, V. Kepe, L.M. Ercoli, P. Siddarth, S. Read, N. Satyamurthy, A. Petric, S.C. Huang, J.R. Barrio, Localization of neurofibrillary tangles and beta-amyloid plaques in the brains of living patients with Alzheimer disease, Am. J. Geriatr. Psychiatry. 10 (2002) 24–35.

[6] G.W. Small, V. Kepe, L.M. Ercoli, P. Siddarth, S.Y. Bookheimer, K.J. Miller, H. Lavretsky, A.C. Burggren, G.M. Cole, H.V. Vinters, P.M. Thompson, S.C. Huang, N. Satyamurthy, M.E. Phelps, J.R. Barrio, PET of brain amyloid and tau in mild cognitive impairment, N. Engl. J. Med. 355 (2006) 2652–2663.

[7] C.A. Mathis, Y. Wang, D.P. Holt, G.F. Huang, M.L. Debnath, W.E. Klunk, Synthesis and evaluation of ^{11}C-labeled 6-substituted 2-arylbenzothiazoles as amyloid imaging agents, J. Med. Chem. 46 (2003) 2740–2754.

[8] W.E. Klunk, H. Engler, A. Nordberg, Y. Wang, G. Blomqvist, D.P. Holt, M. Bergstrom, I. Savitcheva, G.F. Huang, S. Estrada, B. Ausen, M.L. Debnath, J. Barletta, J.C. Price, J. Sandell, B.J. Lopresti, A. Wall, P. Koivisto, G. Antoni, C.A. Mathis, B. Langstrom, Imaging brain amyloid in Alzheimer's disease with Pittsburgh Compound-B, Ann. Neurol. 55 (2004) 306–319.

[9] M. Ono, A. Wilson, J. Nobrega, D. Westaway, P. Verhoeff, Z.P. Zhuang, M.P. Kung, H.F. Kung, ^{11}C-labeled stilbene derivatives as Abeta-aggregate-specific PET imaging agents for Alzheimer's disease, Nucl. Med. Biol. 30 (2003) 565–571.

[10] N.P. Verhoeff, A.A. Wilson, S. Takeshita, L. Trop, D. Hussey, K. Singh, H.F. Kung, M.P. Kung, S. Houle, In-vivo imaging of Alzheimer disease beta-amyloid with [^{11}C]SB-13 PET, Am. J. Geriatr. Psychiatry. 12 (2004) 584–595.

[11] M.P. Kung, C. Hou, Z.P. Zhuang, B. Zhang, D. Skovronsky, J.Q. Trojanowski, V.M. Lee, H.F. Kung, IMPY: an improved thioflavin-T derivative for *in vivo* labeling of beta-amyloid plaques, Brain Res. 956 (2002) 202–210.

[12] A.B. Newberg, N.A. Wintering, C.M. Clark, K. Plossl, D. Skovronsky, J.P. Seibyl, M.P. Kung, H.F. Kung, Use of ^{123}I-IMPY SPECT to differentiate Alzheimer's disease from controls, J. Nucl. Med. 47 (2006) 78P.

[13] Y. Kudo, N. Okamura, S. Furumoto, M. Tashiro, K. Furukawa, M. Maruyama, M. Itoh, R. Iwata, K. Yanai, H. Arai, 2-(2-[2-Dimethylaminothiazol-5-yl]ethenyl)-6-(2-[fluoro]ethoxy)benzoxazole: A novel PET agent for *in vivo* detection of dense amyloid plaques in Alzheimer's disease patients, J. Nucl. Med. 48 (2007) 553–561.

[14] M. Ono, N. Yoshida, K. Ishibashi, M. Haratake, Y. Arano, H. Mori, M. Nakayama, Radioiodinated flavones for *in vivo* imaging of beta-amyloid plaques in the brain, J. Med. Chem. 48 (2005) 7253–7260.

[15] M. Hadjeri, C. Beney, A. Boumendjel, Recent advances in the synthesis of conveniently substituted flavones, quinolones, chalcones and aurones: potential biologically active molecules, Curr. Org. Chem. 7 (2003) 679–689.

[16] Y. Cheng, W.H. Prusoff, Relationship between the inhibition constant (K1) and the concentration of inhibitor which causes 50 per cent inhibition (I50) of an enzymatic reaction, Biochem. Pharmacol. 22 (1973) 3099–3108.

[17] H. Mori, K. Takio, M. Ogawara, D.J. Selkoe, Mass spectrometry of purified amyloid beta protein in Alzheimer's disease, J. Biol. Chem. 267 (1992) 17082–17086.